https://doi.org/10.37434/tpwj2021.09.08

THREE-DIMENSIONAL VISUALIZATION OF THE DETECTED DEFECTS BY EDDY CURRENT COMPUTING TOMOGRAPHY

O.O. Vertiy[1] and **V.M. Uchanin**[2]
[1]National Aerospace University «Kharkiv Aviation Institute»
17 Chkalov Str., 61070, Ukraine. E-mail: alexey.vertiy@gmail.com
[2]G.V. Karpenko Physico-Mechanical Institute of NASU
5 Naukova Str., 79060, Lviv, Ukraine. E-mail: vuchanin@gmail.com

Nondestructive computing tomography methods based on different physical phenomena are reviewed as an effective tool to solve many NDT problems in the context of NDE 4.0 revolution. Eddy current (EC) tomography principle and experimental set-up are presented to demonstrate the possibility to reconstruct tomography images related to the distribution of material electric conductivity. A riveted joint of two aluminium alloy sheets with 2 mm long artificial cracklike defects was selected as an example of complex enough inspected structure. Investigations were carried out with two types of eddy current probes (ECP) application: the first one — the traditional EC probe of absolute type with coaxial driving and sensing coils, and the second — low-frequency double differential EC probe of MDF 1201 type. The set of vertical (orthogonal to the inspected surface) slices for the rivet zone were obtained to demonstrate the effectiveness of EC tomography. The horizontal slices were analyzed to demonstrate the possibility to produce tomography images at different depths. Two-layer structures, consisting of upper sheets with thicknesses from 0 to 8 mm and 5 mm thick lower sheath with a cracklike defect were applied to reconstruct the vertical tomography slices using double differential EC probes. The latter results demonstrate the great depth of evaluation with application of ECP of double differential type and the possibility to estimate the detected defect size and distance from the inspected surface. 34 Ref., 8 Figures.

K e y w o r d s : eddy current (EC) tomography, eddy current probe (EC probe), double differentiation EC probe, electric conductivity, tomography images, slices, riveted joints

The fourth industrial revolution gradually acquires real meaning, as indicated by numerous publications [1, 2]. Fully automated plants, built on Industry 4.0 principles with real-time control of all the processes, are already in operation. The respective government programs are in place in the majority of industrialized countries. Unfortunately, Ukraine is still far behind this global trend, even though some leaders do appear here too [3].

It is obvious that the coming restructuring of industry cannot avoid the need to form new approaches in nondestructive evaluation (NDE) and the world NDE community is already actively discussing this topic, proclaiming formation of the 4th revolution in NDE under the abbreviation of NDE 4.0 (Nondestructive evaluation 4.0) [4, 5]. Reviewing these studies is not the objective of this paper. We will only note that one of the directions in development of NDE 4.0 technologies is automation of testing operations (also using robots) and intellectualization of the control means. We will state with cautious optimism that local specialists on eddy current evaluation have certain achievements in this direction [6–8]. A series of automated systems (including robotic system) have been designed, and new approaches have been developed to processing signals from eddy current probes (ECP) [6–9].

NDE methods, based on tomographic principles of data processing and presentation, can be definitely regarded as NDE 4.0 technologies. The most widely accepted NDE methods, based on probing the evaluated object (EO) by external fields of different nature, are gradually getting tomographic realizations.

The first mathematical tomographic algorithms were used in X-ray radiation range, characterized by an exponential decay law. X-ray computer tomography (CT) allows realization of NDE of OC inner structure by multiple X-ray transmissions in different directions with subsequent processing of the projection data and plotting a 3D distribution of the degree of radiation attenuation. X-ray CT for medical applications was invented for the first time by Godfrey Hounsfield, British inventor, who was granted the respective patent [10] in 1972, and already in 1979, together with Alan Kormak he won the Nobel Prize in physiology and medicine for «Development of computer tomography». And industrial tomography, as an NDE method, emerged already as a projection of the success of medical CT. At present, X-ray CT is the most widely used method of tomographic plotting of images of the internal structure in medicine and industrial NDE [11–14]. This development led to that application of X-ray CT at NDE is regulated by a series of international standards (EN 16016-1(2,3)-1(2,3):2011), starting from 2011.

Achievement in ultrasonic CT became the next tomographic «stronghold», where we can mention the results obtained by scientists of G.V. Karpenko Physico-Mechanical Institute of NASU [15–18]. With time, it was the turn of electric (resistive) and electromagnetic (including eddy current) methods [19–28]. Here, the priority belongs to the results of the representatives of Ukraine, obtained in the Turkish-Ukrainian International Laboratory of High Technologies of «Marmara» Research Center (Hebze, Turkey). Here, theoretical approaches were used, developed earlier for UHF range [20–22]. It is important that in addition to formulation of the theoretical principles, a series of experimental results were derived [19, 23–24], which showed that practical implementation of eddy current tomography (ECT) approaches will allow raising the eddy current NDE method to a fundamentally new level. Note that foreign studies on ECT are still of a theoretical stage, and have not reached the experimental level [28].

The objective of this paper is presentation and generalization of developments on eddy current computational tomography.

Principle of eddy current tomography. Restoring the distribution of specific electric conductivity (SEC) in any EO cross-slice is based on an integral equation of tomography [19–22]:

$$\frac{\hat{\psi}(\nu, y_1)\exp\left(i\gamma_1 y_1\right)}{c_1\left(\nu\right)} = \iint\limits_S K\left(x', y'\right)\exp[-2\pi i(\alpha x' + \beta y')]dx'dy', \tag{1}$$

where $\hat{\psi}\left(\nu, y_1\right)$ is the Fourier-transformation of a complex scattered field $\psi(x, y)$, measured above the surface of the studied environment on the scanning line $y = y_1$; v variable is the spatial frequency; $c_1[\gamma_1(\nu), \gamma_2(\nu)]$ is the complex function of v; γ_1; γ_2, and β are the complex functions of v in the general case; α is the real-valued function of v; $K(x', y')$ is the unknown (sought) normalized distribution of current in S domain (EO transverse slice) that is the scattered field source. The studied domain was limited, so that the integral in equation (1) can be considered in unlimited boundaries. Here, it is taken, that Fourier transformation of the scattered field does exist, as this field is considered in a limited space domain.

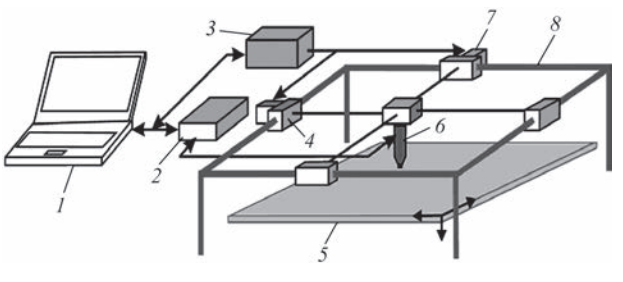

Figure 1. Diagram of experimental set up for eddy current tomography

Solution of this integral equation allows defining $K(x', y')$ function that describes the normalized current distribution in the studied transverse slice, perpendicular to the metal surface, and including the scanning line (vertical slice). $K(x', y')$ function depends on operational frequency (frequency of the probing electromagnetic field). In tomography measurement and reconstruction of $K(x', y')$ function are performed for a certain set of operational frequencies in a specified range. The tomographic image function is the module of the sum of these functions. It enables detecting the inhomogeneity of metal SEC in the vertical slice, including that associated with the presence of defects. Application of tomographic algorithm allows obtaining sufficiently high-quality images of the transverse slices of local (pore type) and extended (cracklike) defects. A set of images in different vertical (orthogonal relative to the surface of the object of inspection) transverse slices allows reconstruction of a 3D image of the studied EO zone.

Experimental set-up for automatic evaluation by the principle of eddy current computing tomography. Experimental set-up (Figure 1) consists of personal computer *1*, eddy current block *2* to determine the signal components in the operational frequency range, control unit *3* with stepping motors *4* and *7* of scanning of ECP *6* along coordinates *X* and *Y*, which are a component of two-coordinate scanner *8*, and studied specimen *5*. Appearance of the set-up with a two-coordinate scanner, installed on the evaluated specimes, is shown in Figure 2.

Personal computer controls the operation of stepping motors of the two-coordinate scanner and eddy current block, records and stores the parameters (amplitude and phase) of ECP signals in discrete points of the evaluated zone at sixteen operational frequencies in the selected range, performs discretization and processing of signals by the developed tomographic algorithm and forms a colour presentation of the obtained results, which reproduces the two-dimensional distribution of SEC in the selected EO slices. Eddy current block functions as a conventional multifrequency flaw detector, which operates ECP of different types (absolute, differential, etc.). Its feature is fast switching of operational frequencies, required for realization of tomographic algorithms, and an improved compensation scheme, which allows widening the dynamic range during processing of ECP output signals. In the reconstructed tomographic images the EO homogeneous region was reproduced by blue colour, the zone of anomaly (defect) — by red colour and the transition zones — by green colour.

Two types of ECP were used for experimental studies. The first is the traditional ECP of absolute type produced by Nortec Company, which consisted of two (driving and sensing) coaxial windings. The features of ECP of this type are described in a review [29], and those of spatial distribution of ECP signal from cracks of different length were analyzed in work [30]. Another, low-frequency double differention ECP of MDF-1201 type was developed at G.V. Karpenko Physico-Mechanical Institute of NASU [31]. ECP of double differentiation consists of two excitation windings connected in series and placed side by side, and two differentially connected sensing windings. Sensing windings are located in the neutral plane, where the electromagnetic field of excitation windings flows in the opposite direction, so that the total electromagnetic field of both the windings is absent, and eddy currents are added, contrarily. Such an ECP has four sensitivity zones for a local defect. Elongated defects form a «quasiabsolute» signal with maximum amplitude directly above the defects, as in the standard ECP of absolute type. A feature of this ECP is the great depth of testing that was reported in a series of publications [31, 32].

Tomographic visualization of defects in the riveted joint. Rivets are the most widely used element of multilayer aircraft structures, which are used for joining the connected skins, reinforcing plates, stringers, etc. At the same time, rivet welds of aircraft structures create the greatest number of stress raisers and thus require greater attention in service. Note that during detect detection in the riveted joint it is necessary to eliminate the effect of the rivet itself, which, essentially also is an admissible, in terms of design, large-sized defect and which creates additional interference signals. Therefore, the task of detecting fatigue cracks (particularly, internal), that form in operation in the riveted joint, is a real challenge for eddy current method developers. Nonetheless, we showed in our research that it is possible to create a range of no-alternative NDE technologies for riveted components on the base of eddy current method, particularly when it is necessary to detect fatigue cracks in the rivet inner layers or under its head [33, 34]. In our experiment, a rivet with a defect was selected to show the capabilities in difficult cases.

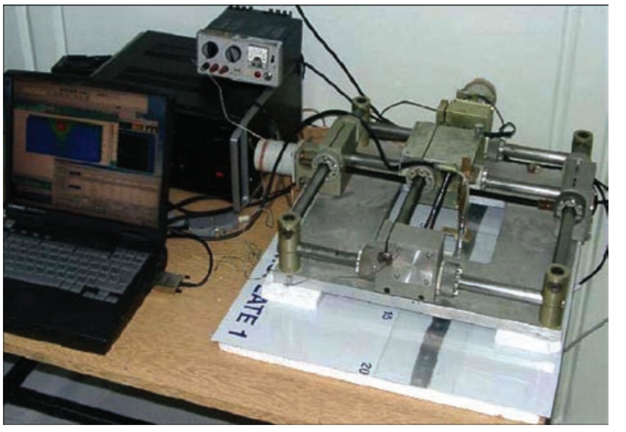

Figure 2. Appearance of an experimental set-up for eddy current tomography

A fragment of an aircraft two-layer skin was used for investigations, which has SEC value equal to 35.4 mS/m, with rows of rivets with artificial cracklike defects, made by electric erosion method. The thickness of each layer of the structure was equal to 2.5 mm. Rivet head diameter was 6 mm, and that of the rivet hole was 5 mm. The scheme of scanning zone of the selected rivet is shown in Figure 3, *a* (side view) and Figure 3, *b* (top view). Rectangular slice of two-dimensional scanning (frame) for an individual rivet was selected equal to 10 mm along coordinate *X* and 15 mm along coordinate *Y* (marked by gray colour in Figure 3). Figure 3, *a* shows that in the selected design the rivets were placed in special recesses, so that a slot formed between the sheath material and the rivet body.

Results obtained with application of traditional ECP of an absolute type. The process of obtaining tomographic images in different slices, corresponding to different scanning lines, and different ECP positions relative to the rivet, respectively, is shown in Figure 4. The numbers denote the coordinates on axes *X* and *Y*. The re-

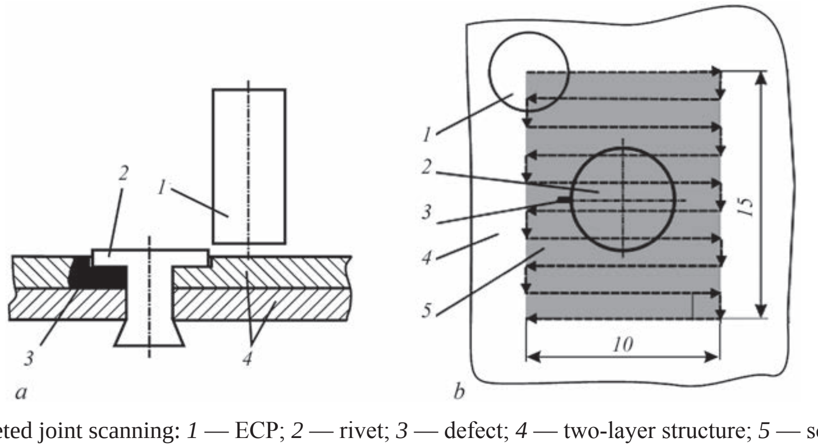

Figure 3. Scheme of riveted joint scanning: *1* — ECP; *2* — rivet; *3* — defect; *4* — two-layer structure; *5* — scanned region

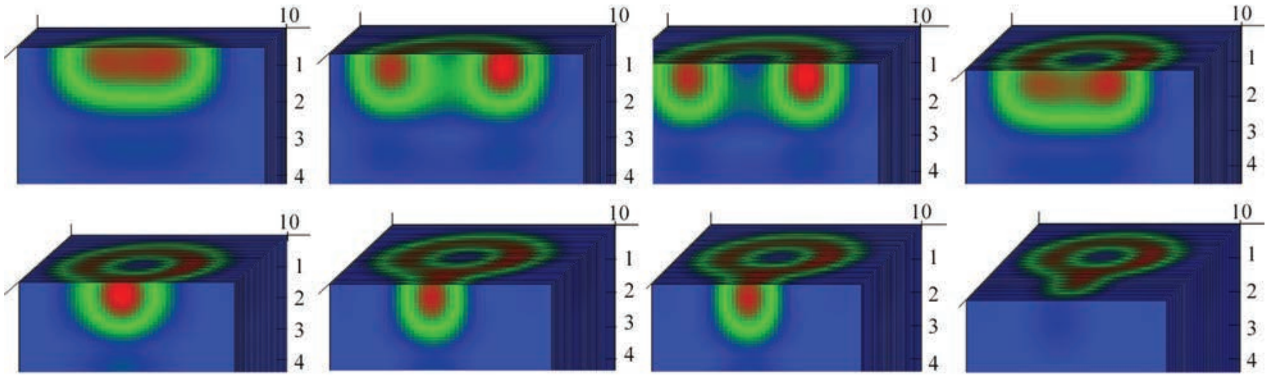

Figure 4. 3D tomographic images of the riveted joint with a defect in different vertical slices

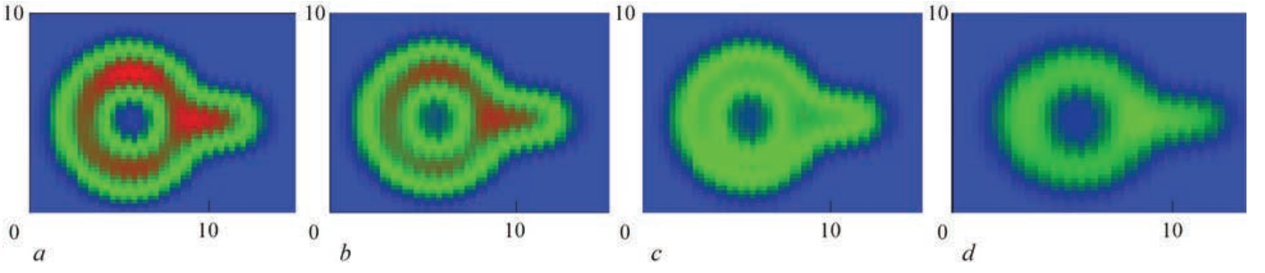

Figure 5. Tomographic reconstruction of the horizontal slice of the riveted joint with a defect at the depth of: 0 (*a*); 0.9 (*b*); 1.2 (*c*), 1.5 mm (*d*), using traditional ECP of an absolute type

sults were obtained by calculation of the amplitude and phase of ECP signal in sixteen operational frequencies in the range from 5 to 50 kHz. The coordinates in the direction normal to the surface (in-depth of the sample) are shown on the right in each image.

After completion of scanning of the selected region, horizontal slices were obtained, which correspond to SEC distribution at different depth. The reconstructed tomographic images are shown in Figure 5.

Developed algorithms allow studying and analyzing different slices of the evaluated zone after completion of the scanning process. As an example, Figure 6 gives a 3D tomographic image of the riveted joint, when the control zone slice was selected along the defect.

The given results also show that when applying the traditional ECP of absolute type in the operational frequency range from 5 to 50 Hz, horizontal tomographic images can be obtained at the depth down to 1.5 mm. Note that similar studies conducted in the operational frequency range from 100 kHz to 1.0 MHz, allow reaching the control depth of just 0.2 mm, that can be readily attributed to a stronger skin-effect.

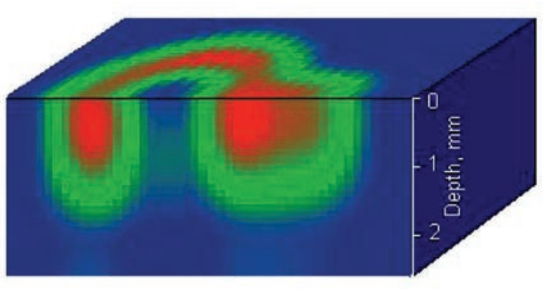

Figure 6. 3D tomographic image of the riveted joint with a vertical slice along the defect

Results of control of the riveted joint, obtained using low-frequency ECP of double differentiation. In the next experiment, a low-frequency ECP of MDF 1201 type was used [31]. Obtained results that characterize the horizontal slices at different depths to 3 mm for defectfree (above) and defective (below) rivets are given in Figure 7. Operational frequencies at application of this ECP were varied in the range of 0.9–10 KHz.

Tomographic images of horizontal slices for a defectfree rivet (Figure 7, *a*, *b*, *c*) have a characteristic four-lobe form, corresponding to the four sensitivity zones of ECP of double differention type [31]. Presence of a cracklike defect distorts the four-lobe image, characteristic for a defectfree rivet. The image becomes asymmetric and one lobe disappears. Such distortions were observed during traditional visualization of the results of riveted joint testing, when the 2D distribution of ECP signal was recorded on electrochemical paper [33]. Note that the testing depth here reached 3 mm that confirms the great depth of testing with application of this ECP.

Vertical slices of electric conductivity distribution from subsurface defects of different depth. Low-frequency ECP of MDF 1201 type was also used to conduct experiments with layered specimens with cracklike defects in the internal layers. Recall that for elongated defects of the type of cracks the signal from ECP of double differention type is of a

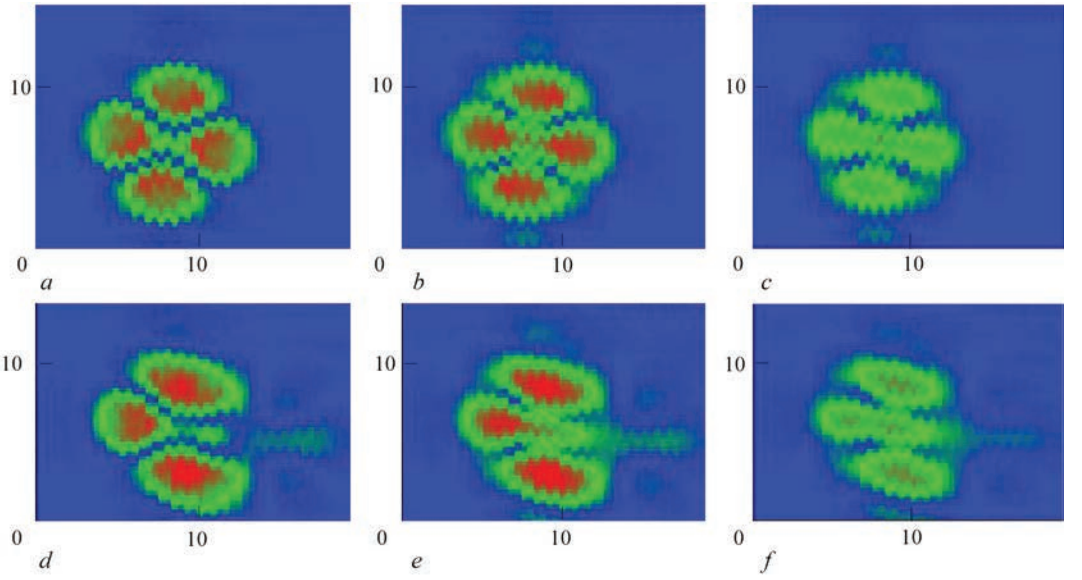

Figure 7. Tomographic image of a horizontal slice at different depths: 0 (*a*, *d*); 2.0 (*b*, *e*); 3.0 mm (*c*, *f*) during eddy current scanning of the zone of defectfree rivet (*a*, *b*, *c*) and rivet with a crack (*d*, *e*, *f*)

«quasiabsolute» nature that affects the obtained tomographic images. The crack was simulated by a butt of two aluminium plates 5.0 mm thick, which were placed on a base aluminium plate 5.0 mm thick. The specimen was covered from above by plates 1.5; 2.5; 5.0; 6.5 and 8.0 mm thick to change the defect depth. Layered specimens were scanned by ECP parallel to the surface by a linear trajectory 39.6 mm long. In order to reconstruct the vertical (normal to the surface) specimen slice, ECP signals were recoded in sixteen operational frequencies in the range of 0.9–10 KHz in each point every 0.6 mm along the scanning line. In the tomographic reconstructed images the homogeneous region was reproduced by blue colour, anomalous zone — by the red colour and the transition zones were shown by green colour. In the tomographic images of vertical slice of the layered specimens (Figure 8) the coordinates along the line of scanning over the specimen surface are shown on top in mm, and on the right are the coordinates in the direction normal from the surface (in-depth of the sample).

In the tomographic images of vertical slice, the anomalous zones that correspond to the defect, are marked by the red colour, their upper edge corresponding to the defect depth (upper plate thickness), which is counted by the right scale. The length of the red anomalous zone along the vertical in-depth of the metal corresponds to defect height (5.0 mm). An exception is the tomographic image of the specimen slice with the surface defect (without upper plate) (Figure 8, *a*), in which the anomalous zone separated into two regions. It is attributable to existence of side maximums for large-sized defects in

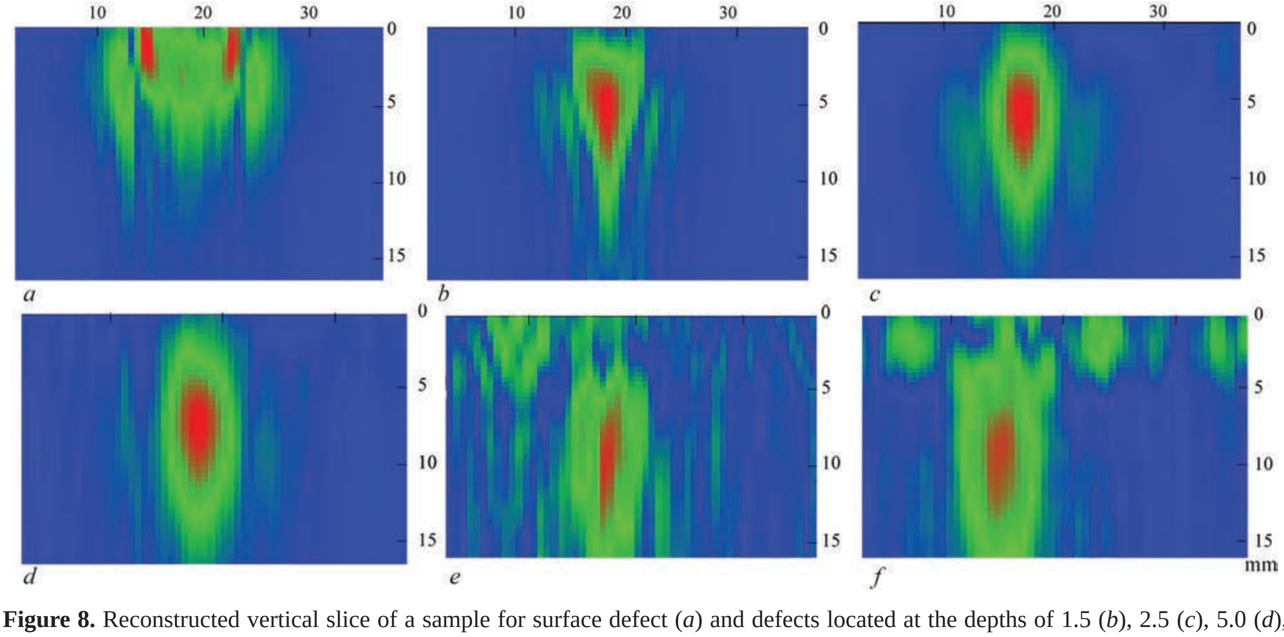

Figure 8. Reconstructed vertical slice of a sample for surface defect (*a*) and defects located at the depths of 1.5 (*b*), 2.5 (*c*), 5.0 (*d*), 6.5 (*e*), 8.0 mm (*f*)

ECP of double differention type. However, the vertical boundary of the red region in the image starts from the specimen surface, as could be anticipated. With increase of the defect depth, large green regions appear in the tomographic images that is related to greater sensitivity of inspection system, and interference level, accordingly. However, the red anomalous zone allows reliably identifying the defect, which is located at down to 8.0 mm depth. Moreover, the position of the defect lower edge is clearly visible, which for the deepest-lying defect corresponds to 13 mm distance from the surface.

The given results are indicative of the principal possibility of quantitative eddy current evaluation with assessment of the detected defect parameters, based on tomographic approaches. Moreover, the great depth of testing using ECP of MDF 1201 type was confirmed.

Conclusions

1. A brief review of nondestructive methods of computer tomography is given, based on different physical phenomena, as an effective technique to solve numerous NDE problems in the context of NDE 4.0 revolution.

2. ECT principle and experimental set-up are presented for reconstruction of tomographic images, related to distribution of material electric conductivity.

3. Two ECP types were used for investigations: the first is a traditional ECP of absolute type with a coaxial sensing and driving windings, and the second is a low-frequency ECP of double differentiation.

4. ECT studies were performed on a two-layer specimen that consists of two plates of an aluminium alloy with rivets and 2 mm cracklike defects. A set of vertical slices (orthogonal relative to the inspected surface) were obtained for the riveted joint, which demonstrated ECT effectiveness. Tomographic images of horizontal slices at different depth were also analyzed.

5. Reconstruction of vertical tomographic slices with application of ECP of double differentiation was performed, using a multilayered structure, which consisted of an upper skin 0–8 mm thick and cracklike defects in the lower layer. Obtained results showed the great inspection depth at application of ECP of this type and possibility of assessment of the size of the detected defect and its distance to the inspected surface.

6. Application of ECT principles will allow raising the eddy current evaluation to a fundamentally new level. Resuming ECT investigations and developments can be regarded as a national priority.

The authors would like to express their gratitude to academician Z.T. Nazarchuk, who promoted organization of joint research and cooperation of the authors.

1. Liao, Y., Deschamps, F., Loures, E.F.R., Ramos, L.F.P. (2017) Past, present and future of Industry 4.0 — a systematic literature review and research agenda proposal. *Intern. J. of Production Research,* **55**(12), 3609–3629. http://doi.org/10.1080/00207543.2017.1308576.
2. Drath, R., Horch, A. (2014) Industrie 4.0: Hit or Hype. *IEEE Industrial Electronics Magazine*, **8**(2), 56–58. http://doi.org/10.1109/mie.2014.2312079.
3. Yurchak, A. (2019) Far from the neighbours: why Ukraine lags behind in the sphere of industrial development 4.0. *Ekonomichna Pravda.* https://www.epravda.com.ua/rus/columns/2019/11/5/653346.
4. Singh, R. (2019) The next revolution in nondestructive testing and evaluation: What and how. *Materials Evaluation*, **77**(1), 45–50.
5. Vrana, J. (2020) NDE Perception and emerging reality: NDE 4.0 value extraction, *Materials Evaluation,* **78**(7), 835–851.
6. Naida, V.L., Uchanin, V.N., Mozhukhin, A.A. et al. (2008) Development of elements of a system of automated eddy current testing of collector bridges in nuclear power plants. *Tekh. Diagnost. i Nerazrush. Kontrol*, **3**, 21–24 [in Russian].
7. Lutcenko, G., Uchanin, V., Mischenko, V., Opanasenko, A. (2012) Eddy currents versus magnetic particles. In: *Proc. of 18th World Conf. on Nondestructive Testing,* Durban, www.ndt.com.
8. Dolinenko, V.V., Shapovalov, E.V., Skuba, T.G. et al. (2017) Robotic system of non-destructive eddy-current testing of complex geometry products. *The Paton Welding J*., **5–6**, 60–67. http://doi.org/10.15407/as2017.06.10.
9. Lysenko, Ju., Eremenko, V., Kuts, Yu. et al. (2020) Advanced signal processing methods for inspection of aircraft structural materials. *Transact. on Aerospace Research*, **2**(259), 27–35. http://doi.org/10.2478/tar-2020-0008.
10. Hounsfield, G. N. (1972) A *method and apparatus for examination of a body by radiation such as X-ray or gamma radiation*. British Pat. 1283915. British Patent Office, London.
11. Vajnberg, E.I., Klyuev, V.V., Kurozaev, V.P. (1986) *Industrial X-ray computed tomography*: Book. Devices for non-destructive testing of materials and products: Refer. book. Ed. by V.V. Klyuev. 2nd Ed., Moscow, Vol. 1 [in Russian].
12. Vajnberg, E.I., Kazak, I.A., Kurozaev, V.P. (1981) Reconstruction of internal space structure of objects by integral projections in real time. *DAN SSSR*, **257**(1), 89–94 [in Russian].
13. Reimers, P., Goebbels, J. (1983) New possibilities of nondestructive evaluation by X-ray computed tomography. *Materials Evaluation*, **42**(6), 732–737
14. Maire, E., Buffiere, J., Salvo, L. et al. (2001) On the application of X-ray microtomography in the field of materials science. *Advanced Engineering Materials*, **3**(8), 539–546.
15. Nazarchuk, Z.T., Koshovy, V.V., Krivin, E.V., Romanyshyn, I.M. (1999) Ultrasonic tomography, technologies for NDT and monitoring of material degradation. In: *Proc. Joint EC IAEA Specialists Meeting on NDT Methods for Monitoring Degradation*. Petten, The Netherlands, 79–89.
16. Koshovyy, V. V., Nazarchuk, Z. T. (2001) Estimating the predefective state of a material using methods of ultrasonic computerized tomography. *Materials Sci.*, **37**(2), 279–293.
17. Koshevoj, V.V., Romanishin, I.M., Romanishin, R.I., Sharamaga, R.V. (2010) Ultrasonic computer tomography based

on recording of a signal scattered by material structure. Pt 1. *Tekh. Diagnost. i Nerazrush. Kontrol*, **2**, 37–42 [in Russian].
18. Koshevoj, V.V., Romanishin, I.M., Romanishin, R.I., Sharamaga, R.V. (2010) Ultrasonic computer tomography based on recording of a signal scattered by material structure. Pt 2. *Tekh. Diagnost. i Nerazrush. Kontrol*, **3**, 19–24 [in Russian].
19. (2011) *Subsurface sensing*. Ed. by A.S.Turk, A.K., Hocaoglu, A.A. Vertiy, John Wiley & Sons, Inc.
20. Vertiy, A., Gavrilov, S., Voynovskyy, I., Stepanyuk, V. (2002) The millimeter wave tomography application for the subsurface imaging. *Int. J. of Infrared and Millimeter Waves*. **23**(10), 1413–1444.
21. Gavrilov, S.P., Vertiy, A.A. (1997) Application of tomography method in millimeter wavelengths band: I. Theoretical. *Int. J. Infrared Millimeter Waves*, **18**(9), 1739–1760.
22. Vertiy, A.A., Gavrilov, S.P. (1997) Application of tomography method in millimeter wavelengths band: II. Experimental. *Int. J. Infrared Millimeter Waves*, **18**(9), 1761–1781.
23. Vertiy, A., Gavrilov, S., Voynovskyy, I. et al. (2004) Subsurface imaging by deep penetrating eddy current tomography. *Fizychni Metody ta Zasoby Kontrolyu Seredovyshch, Materialiv ta Vyrobiv*, **9**, 123–127 [in Russian].
24. Vertiy, A.A., Gavrilov, S.P., Voynovskyy, I.V. et al. (2004) Deep penetrating eddy current tomography for subsurface imaging. In: *Proc. of 10th Int. Workshop on Electromagnetic Evaluation.* Michigan, USA. 91–92.
25. Tamburrino, A. Rubinacci, G. (2002) A new non-iterative inversion method for electrical resistance tomography. *Inverse Problems*, **18**(6), 1809–1829.
26. Tamburrino, A., Soleimani, M. (2006) Shape reconstruction in magnetic induction tomography using multifrequency data. *Int. J. of Informaton and Systems Sci.*, **2**(3), 343–353.
27. Tamburrino, A., Rubinacci, G., Soleimani, M., Lionheart, W. (2003) Non iterative inversion method for electrical resistance, capacitance and inductance tomography. In: *3rd World Congress on Industrial Process Tomography*, Banff, Canada, 233–238.
28. Tamburrino, A., Rubinacci, G. (2006) Fast methods for quantitative eddy-current tomography of conductive materials. *IEEE Transact. on Magnetics*, 42(8), 2017–2028.
29. Uchanin, V.N. (2010) Eddy current surface probes: Expanded classification, comparative analysis and characteristic examples of realization. (Review). *Tekh. Diagnost. i Nerazrush. Kontrol*, **4,** 24–29 [in Russian].
30. Uchanin, V.M. (2007) Specific features of the space distribution of the signal of an eddy-current converter caused by cracks of different lengths. *Materials Sci.*, **43**, 591–595. http://doi.org/10.1007/s11003-007-0068-2.
31. Uchanin, V.M. (2013) *Eddy-current* surface probes *of double differention type*. Lviv, Spolom [in Ukrainian].
32. Mook, G., Hesse, J., Uchanin, V. (2007) Deep penetrating eddy currents and probes. *Materials Testing*, **49**(5), 258–264. http://doi.org/10.3139/120.100810.
33. Uchanin, V. (2006) Eddy current methods of detection of defects in the zone of rivets of multilayer aircraft structures. *Tekh. Diagnost. i Nerazrush. Kontrol*, **2**, 3–12 [in Russian].
34. Uchanin, V. (2020) Detection of the fatigue cracks initiated near the rivet holes by eddy current inspection techniques. *Transact. on Aerospace Research*, **1**(258), 47–58. http://doi.org/10.2478/tar-2020-0010.

Received 18.03.2021